Numerical Realization of Unsteady Solutions for the 2D Boussinesq Paradigm Equation in a moving frame coordinate system

Christo I. Christov
Dept. of Mathematics, University of Louisiana at Lafayette, USA

Daniela Vasileva
Institute of Mathematics and Informatics, Bulgarian Academy of Sciences

1. Motivation
2. Numerical Method
3. Numerical Results
4. Conclusions

Motivation

- Boussinesq equation is the first model for surface waves in shallow fluid layer that accounts for both nonlinearity and dispersion. The balance between the steepening effect of the nonlinearity and the flattening effect of the dispersion maintains the shape of the waves;

  J. V. Boussinesq, Théorie des ondes et des remous qui se propagent le long d'un canal rectangulaire horizontal, en communiquant au liquide contenu dans ce canal des vitesses sensiblement pareilles de la surface au fond, Journal de Mathématiques Pures et Appliquées 17 (1872) 55–108.

- In the 60s it was discovered that these permanent waves can behave in many instances as particles and they were called *solitons* by Zabusky and Kruskal;

  N. J. Zabusky, M. D. Kruskal, Interaction of 'solitons' in collisionless plasma and the recurrence of initial states, Phys. Rev. Lett. 15 (1965) 240–243.

- A plethora of deep mathematical results have been obtained for solitons in the 1D case, but it is of crucial importance to investigate also the 2D case, because of the different phenomenology and the practical importance;

- The accurate derivation of the Boussinesq system combined with an approximation, that reduces the full model to a single equation, leads to the Boussinesq Paradigm Equation (BPE)

$$u_{tt} = \Delta \left[u - F(u) + \beta_1 u_{tt} - \beta_2 \Delta u \right], \quad F(u) := \alpha u^2,$$

  u is the surface elevation, $\beta_1 > 0$, $\beta_2 > 0$ - dispersion coefficients, $\alpha > 0$ - amplitude parameter, $\beta_2 = \alpha = 1$ without loosing of generality;

  C. I. Christov, An energy-consistent Galilean-invariant dispersive shallow-water model, Wave Motion 34 (2001) 161–174.

- 2D BPE admits stationary translating soliton solutions, which can be constructed using either finite differences, perturbation technique, or Galerkin spectral method;

  M. A. Christou, C. I. Christov, Fourier-Galerkin method for 2D solitons of Boussinesq equation, Math. Comput. Simul. 74 (2007) 82–92.

  J. Choudhury, C. I. Christov, 2D solitary waves of Boussinesq equation, ISIS Intl. Symposium on Interdisciplinary Science, Natchitoches, 2004, APS Conference Proceedings 755 (2005), Washington D.C., 85–90.

  C. I. Christov, J. Choudhury, Perturbation solution for the 2D Boussinesq equation. Mech. Res. Commun., 38 (2010), 274–281

  C. I. Christov, Numerical implementation of the asymptotic boundary conditions for steadily propagating 2D solitons of Boussinesq type equations, Math. Comp. Simulat. Appeared online August 10, 2010

- It is of utmost importance to unvestigate the properties of these solutions when they are allowed to evolve in time, i.e., what is their behaviour when used as initial conditions for time-dependent computations of the Boussinesq equation;

- To obtain reliable knowlegde about the time evolution of the stationary soliton solutions, it is imperative to develop different techniques for solving of the unsteady 2D BPE; Some results in

  A. Chertock, C. I. Christov, A. Kurganov, Central-upwind schemes for the Boussinesq paradigm equation. Computational Sci. & High Performance Computing IV, NNFM, 113 (2011), 267–281

  C.I. Christov, N. Kolkovska, D. Vasileva, On the Numerical Simulation of Unsteady Solutions for the 2D Boussinesq Paradigm Equation, Proc. NMA'10 Conference, Lecture Notes Computer Science, 6046 (2011), 386–394

  C.I. Christov, N. Kolkovska, D. Vasileva, Numerical Investigation of Unsteady Solutions for the 2D Boussinesq Paradigm Equation. Proc. BGSIAM10 (5th Annual Meeting of the Bulgarian section of SIAM, 2010, Sofia)

- The moving frame coordinate system, presented here, allows us to keep the localized structure in the center of coordinate system reducing the effects of the reflection from the boundary when the structure approaches one of them.

Numerical method

We introduce the following new dependent function

$$v(x,y,t) := u - \beta_1 \Delta u.$$

and get the following equation for v

$$v_{tt} = \frac{\beta_2}{\beta_1}\Delta v + \frac{\beta_1 - \beta_2}{\beta_1^2}(u - v) - \alpha \Delta F(u).$$

We set $z := y - ct$, where c is the velocity of the stationary propagating soliton and obtain the following equation for $w(x,z,t) := v(x, z + ct, t)$

$$w_{tt} - 2cw_{tz} + c^2 w_{zz} = \frac{\beta_2}{\beta_1}\Delta w + \frac{\beta_1 - \beta_2}{\beta_1^2}(u - w) - \alpha \Delta F(u).$$

The following implicit time stepping scheme can be designed

$$\begin{aligned}
\frac{w_{ij}^{n+1} - 2w_{ij}^n + w_{ij}^{n-1}}{\tau^2} - c\frac{V_z[w_{ij}^{n+1} - w_{ij}^{n-1}]}{\tau} + \frac{c^2}{2}\Lambda_z[w_{ij}^{n+1} + w_{ij}^{n-1}] &= \frac{\beta_2}{2\beta_1}\Lambda[w_{ij}^{n+1} + w_{ij}^{n-1}] \\
&+ \frac{\beta_1 - \beta_2}{2\beta_1^2}[u_{ij}^{n+1} - w_{ij}^{n+1} + u_{ij}^{n-1} - w_{ij}^{n-1}] - \Lambda G(u_{ij}^{n+1}, u_{ij}^{n-1}); \\
u_{ij}^{n+1} - \beta_1 \Lambda u_{ij}^{n+1} &= v_{ij}^{n+1}, \quad i = 0, \ldots, N_x + 1, j = 0, \ldots, N_y + 1.
\end{aligned}$$

τ is the time increment, the nonlinear term

$$G(u_{ij}^{n+1}, u_{ij}^{n-1}) = \left[(u_{ij}^{n+1})^2 + u_{ij}^{n+1}u_{ij}^{n-1} + (u_{ij}^{n-1})^2\right]/3$$

is linearized with Picard method, i.e., using successive iterations.

$\Lambda = \Lambda^{xx} + \Lambda^{zz}$ is a difference approximation of the Laplace operator Δ on a non-uniform grid

$$\Lambda^{xx}\phi_{ij} = \frac{2\phi_{i-1j}}{h^x_{i-1}(h^x_i + h^x_{i-1})} - \frac{2\phi_{ij}}{h^x_i h^x_{i-1}} + \frac{2\phi_{i+1j}}{h^x_i(h^x_i + h^x_{i-1})} = \frac{\partial^2\phi}{\partial x^2}\Big|_{ij} + O(|h^x_i - h^x_{i-1}|),$$

$$\Lambda^{zz}\phi_{ij} = \frac{2\phi_{ij-1}}{h^z_{j-1}(h^z_j + h^z_{j-1})} - \frac{2\phi_{ij}}{h^z_i h^z_{i-1}} + \frac{2\phi_{ij+1}}{h^z_j(h^z_j + h^z_{j-1})} = \frac{\partial^2\phi}{\partial z^2}\Big|_{ij} + O(|h^z_j - h^z_{j-1}|),$$

and V_z is a difference approximation of $\frac{\partial}{\partial z}$

$$V_z\phi_{ij} := \frac{h^z_{j-1}\phi_{ij+1}}{h^z_j(h^z_j + h^z_{j-1})} - \frac{h^z_i\phi_{ij-1}}{h^z_{j-1}(h^z_j + h^z_{j-1})} - \frac{(h^z_j - h^z_{j-1})\phi_{ij}}{h^z_i h^z_{j-1}} = \frac{\partial\phi}{\partial z}\Big|_{ij} + O(|h^z_j - h^z_{j-1}|).$$

Another way to approximate w_{zt} for $C > 0$ is the following "upwind" approximation

$$w_{zt} = \frac{w^{n+1}_{ij+1} - w^{n+1}_{ij} - w^n_{ij+1} + w^n_{ij}}{2\tau h^z_j} + \frac{w^n_{ij} - w^n_{ij-1} - w^{n-1}_{ij} + w^{n-1}_{ij-1}}{2\tau h^z_{j-1}} + O(|h^z_j - h^z_{j-1}| + \tau^2).$$

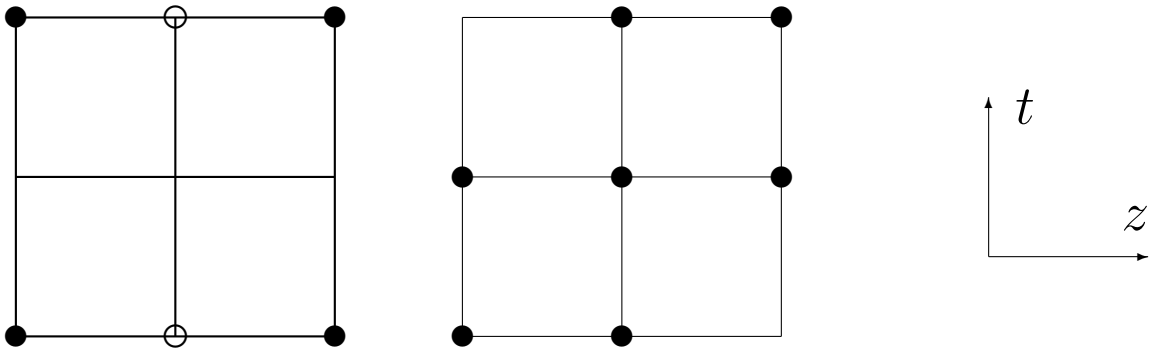

Thus, we have two *coupled* equations for the two unknown grid functions $u^{n+1}_{ij}, w^{n+1}_{ij}$.

We use the following non-uniform grid in the x- and z-directions:

$$
\begin{aligned}
x_i &= \sinh[\hat{h}_1 i],\ x_{N_x+1-i} = -x_i,\ i = \frac{N_x+1}{2}+1,\ldots,N_x+1,\ x_{\frac{N_x+1}{2}} = 0,\\
z_j &= \sinh[\hat{h}_2 j],\ z_{N_z+1-j} = -z_j,\ j = \frac{N_z+1}{2}+1,\ldots,N_y+1,\ y_{\frac{N_z+1}{2}} = 0,
\end{aligned}
$$

where $\hat{h}_1 = D_1/N_x$, $\hat{h}_2 = D_2/N_z$ and D_1, D_2 are selected in a manner to have large enough computational region. For a smooth distribution of the nonuniform grid (as the one considered here) one has

$$
O(|h_i^x - h_{i-1}^x|) \approx \frac{\partial h^x}{\partial x} O(|h_{i-1}|^2) = O(|h_{i-1}|^2).
$$

The boundary conditions can be set equal to zero, because of the localization of the wave profile.

For smaller computational box - asymptotic boundary conditions can be formulated as

$$
x\frac{\partial u}{\partial x} + z\frac{\partial u}{\partial z} \approx -2u, \quad x\frac{\partial w}{\partial x} + z\frac{\partial w}{\partial z} \approx -2w, \qquad \sqrt{x^2+z^2} \gg 1.
$$

$$
\begin{aligned}
u_{iN_z+1}^{n+1} &= u_{iN_z-1}^{n+1} + \frac{h_{N_z}^z + h_{N_z-1}^z}{z_{N_z}}\Big[-2u_{iN_z}^{n+1} - \frac{x_i}{h_i^x + h_{i-1}^x}(u_{i+1N_z}^{n+1} - u_{i-1N_z}^{n+1})\Big], \quad i = 0,\ldots,N_x,\\
u_{N_x+1j}^{n+1} &= u_{N_x-1j}^{n+1} + \frac{h_{N_x}^x + h_{N_x-1}^x}{x_{N_x}}\Big[-2u_{N_xj}^{n+1} - \frac{z_j}{h_j^z + h_{j-1}^z}(u_{N_x,j+1}^{n+1} - u_{N_x,j-1}^{n+1})\Big], \quad j = 0,\ldots,N_z.
\end{aligned}
$$

The coupled system of equations is solved by the Bi-Conjugate Gradient Stabilized Method with ILU preconditioner.

Numerical experiments

We use the following best fit approximation for the shape of the stationary propagating soliton with velocity c

C. I. Christov, J. Choudhury, Perturbation solution for the 2D Boussinesq equation. Mech. Res. Commun., 38 (2010), 274–281

$$u^s(x,z;c) = f(x,z) + c^2\left[(1-\beta_1)g_a(x,z) + \beta_1 g_b(x,z)\right] + c^2\left[(1-\beta_1)h_1(x,z) + \beta_1 h_2(x,z)\right]\cos(2\arctan(z/x).$$

$$f(x,z) = \frac{2.4(1+0.24r^2)}{\cosh(r)(1+0.095r^2)^{1.5}}, \quad g_a(r) = -\frac{1.2(1-0.177r^{2.4})}{\cosh(r)(1+0.11r^{2.1})}, \quad g_b(r) = -\frac{1.2(1+0.22r^2)}{\cosh(r)(1+0.11r^{2.4})},$$

$$h_i(x,z) = \frac{a_i r^2 + b_i r^3 + c_i r^4 + v_i r^6}{1 + d_i r + e_i r^2 + f_i r^3 + g_i r^4 + h_i r^5 + q_i r^6 + w_i r^8}, \quad r(x,z) = \sqrt{x^2+z^2}, \quad \theta(x,y) = \arctan(z/x),$$

$a_1 = 1.03993,\ a_2 = 31.2172,\ b_1 = 6.80344,\ b_2 = -10.0834,\ c_1 = -0.22992,\ c_2 = 3.97869,\ d_1 = 12.6069,\ d_2 = 77.9734,$

$e_1 = 13.5074,\ e_2 = -76.9199,\ f_1 = 2.46495,\ f_2 = 55.4646,\ g_1 = 2.45953,\ g_2 = -12.9335,\ h_1 = 1.03734, h_2 = 1.0351,$

$q_1 = -0.0246084,\ q_2 = 0.628801,\ v_1 = 0.0201666,\ v_2 = -0.0290619,\ w_1 = 0.00408432,\ w_2 = -0.00573272.$

In the examples below $u^s(x,z;c)$ for $\beta_1 = 3$ is taken as initial data for $t = 0$ and the second initial condition may be chosen as

$$\partial u/\partial t = 0, \quad t = 0, \quad \text{or} \quad u(x,z,-\tau) = u^s(x,z;c).$$

Example 1. The first case is for a phase speed $c = 0.27$. The grid has 161×161 points in the region $[-20, 20]^2$, $\tau = 0.1$. For $t < 10$ the solution stays near the center of the moving frame coordinate system and behaves like a soliton, i.e., preserves its shape, although its maximum slightly decreases. For larger times the solution transforms into a diverging propagating wave. The values of the maximum of the solution $u_{\max}$ and the trajectory of the maximum $y_{\max}$ are shown in Fig.1. The results in the next figures are for fixed coordinates (Fig.2), for moving frame with upwind approximation of w_{tz} (Fig.3), with central differences approximation of w_{tz} (Fig.4), for finer grid with 321×321 points and $\tau = 0.05$ (Fig.5) for larger computational region - 641×641 points in $[-200, 200]^2$, $\tau = 0.1$ (Fig.6) and for larger times in the larger region (Fig.7).

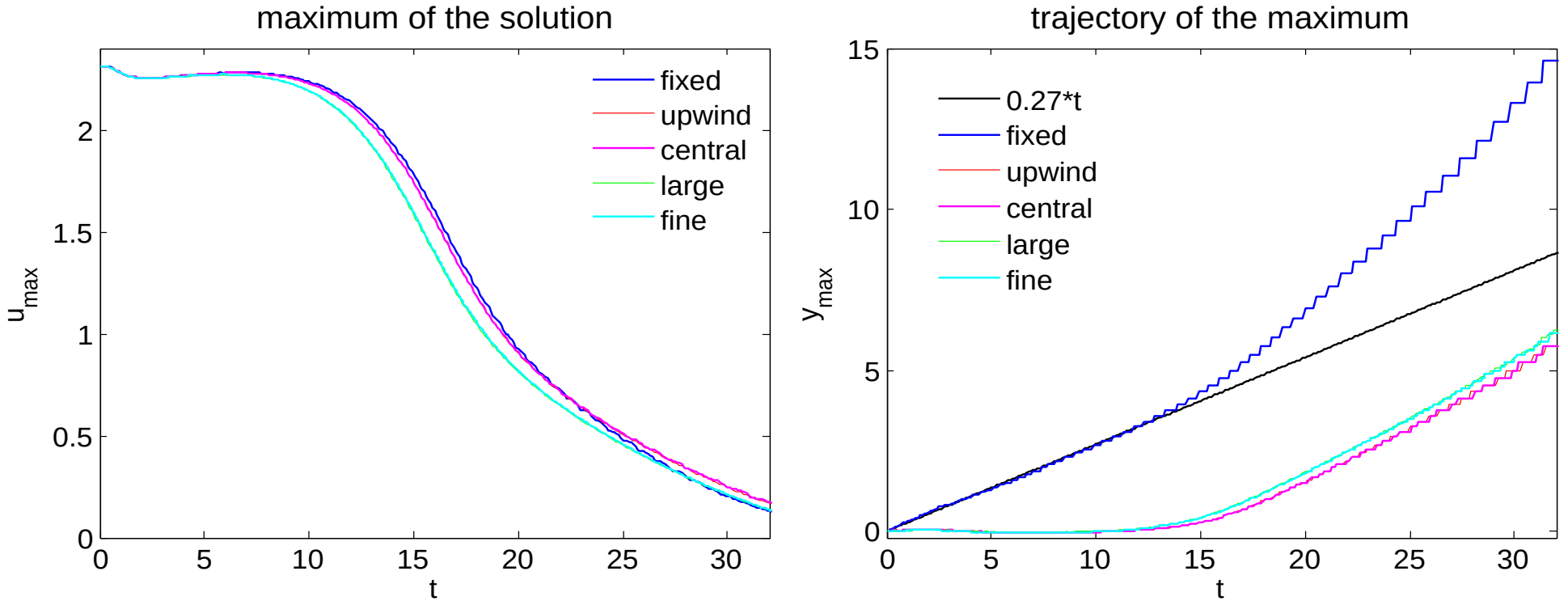

Figure 1: Evolution of the solution for $c = 0.27$ – the values and the trajectory of the maximum

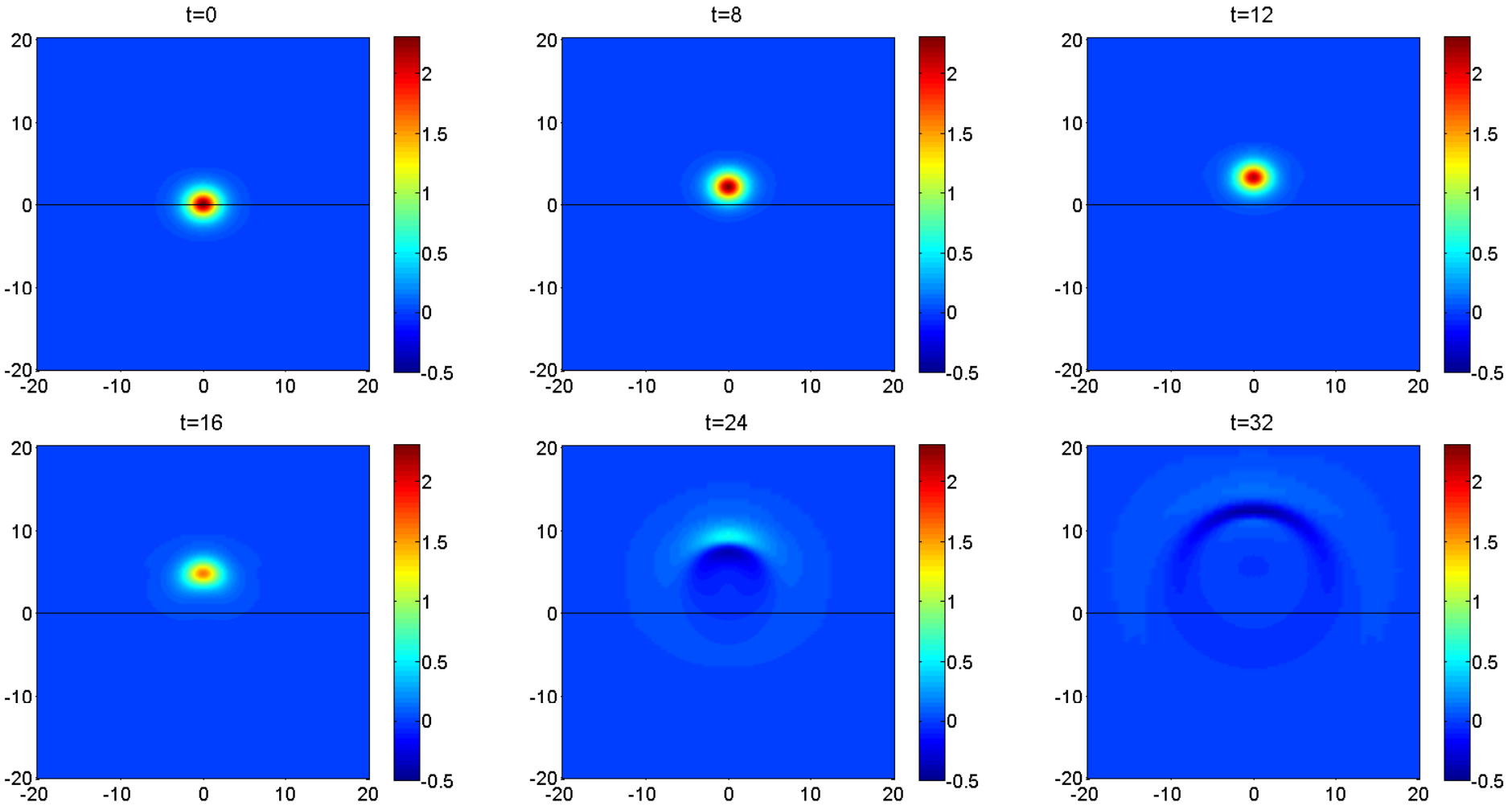

Figure 2: Evolution of the solution for $c = 0.27$, fixed coordinate system, grid with 161×161 points in $[-20, 20]^2$, $\tau = 0.1$.

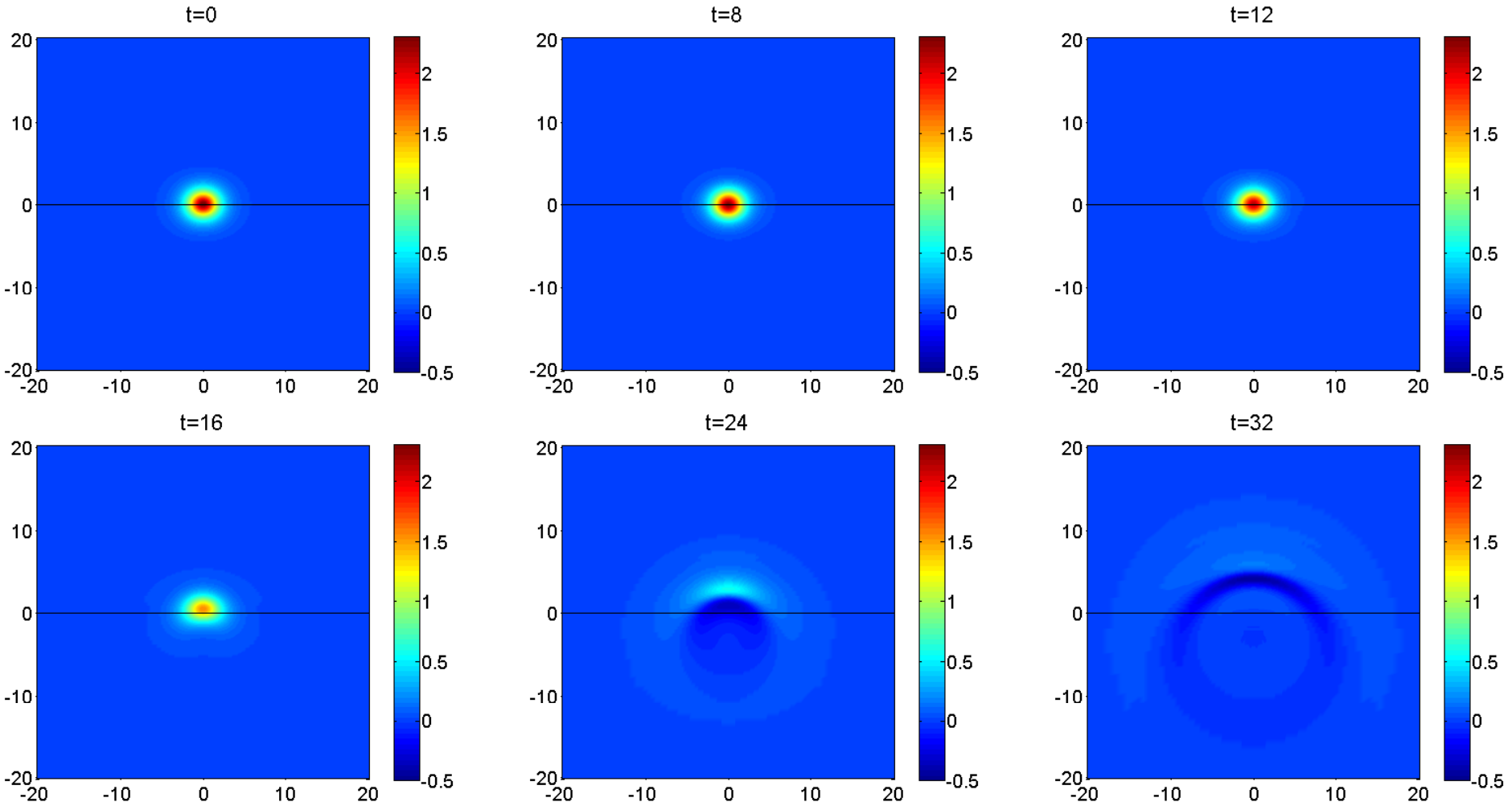

Figure 3: Evolution of the solution for $c = 0.27$, moving frame, upwind approximation of w_{tz}, grid with 161×161 points in $[-20, 20]^2$, $\tau = 0.1$.

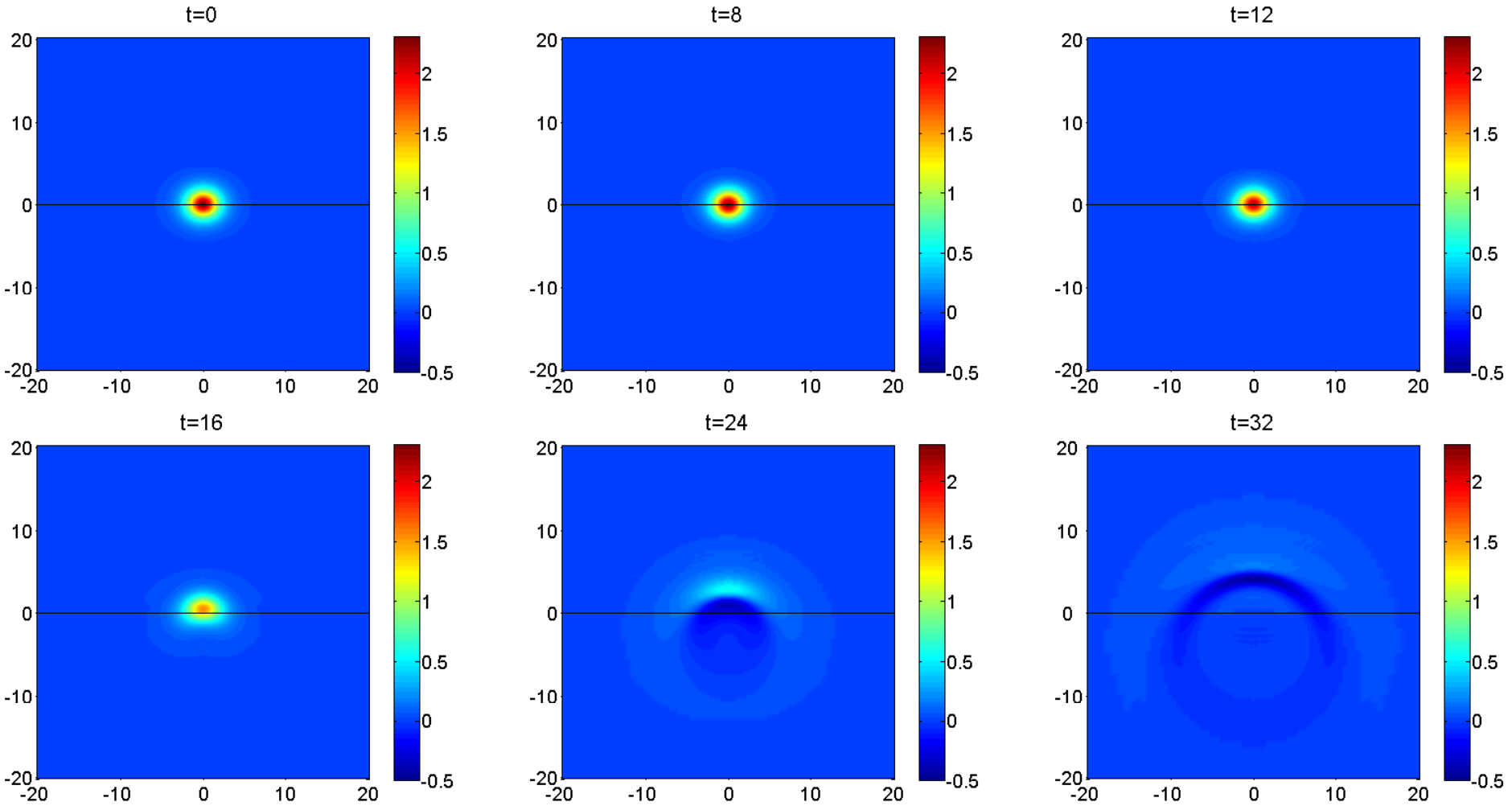

Figure 4: Evolution of the solution for $c = 0.27$, moving frame, central differences approximation of w_{tz}, grid with 161×161 points in $[-20, 20]^2$, $\tau = 0.1$.

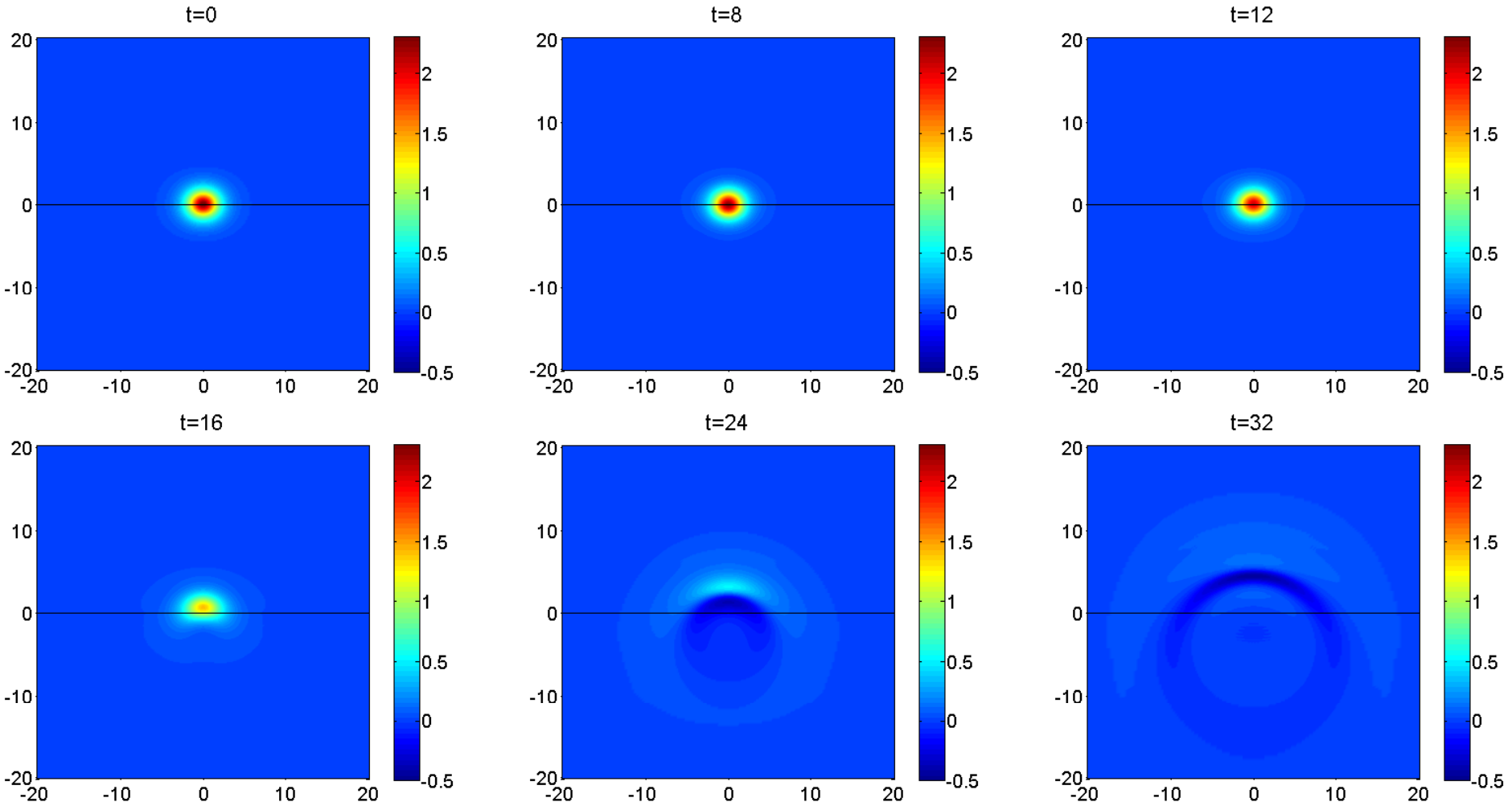

Figure 5: Evolution of the solution for $c = 0.27$, moving frame, central differences approximation of w_{tz}, finer grid with 321×321 points in $[-20, 20]^2$, $\tau = 0.05$.

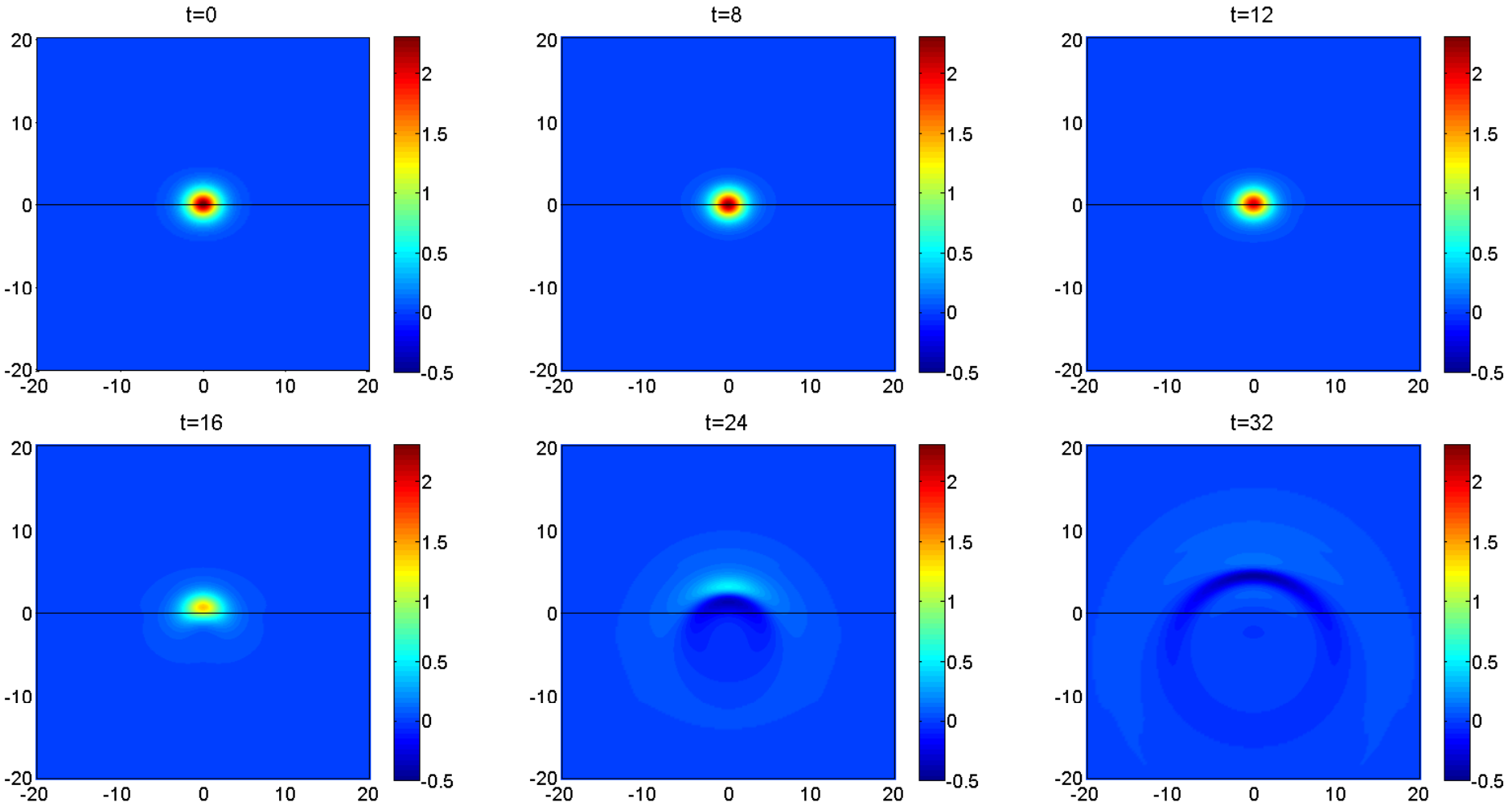

Figure 6: Evolution of the solution for $c = 0.27$, moving frame, central differences approximation of w_{tz}, larger region $[-200, 200]^2$, grid with 641×641 points, $\tau = 0.1$.

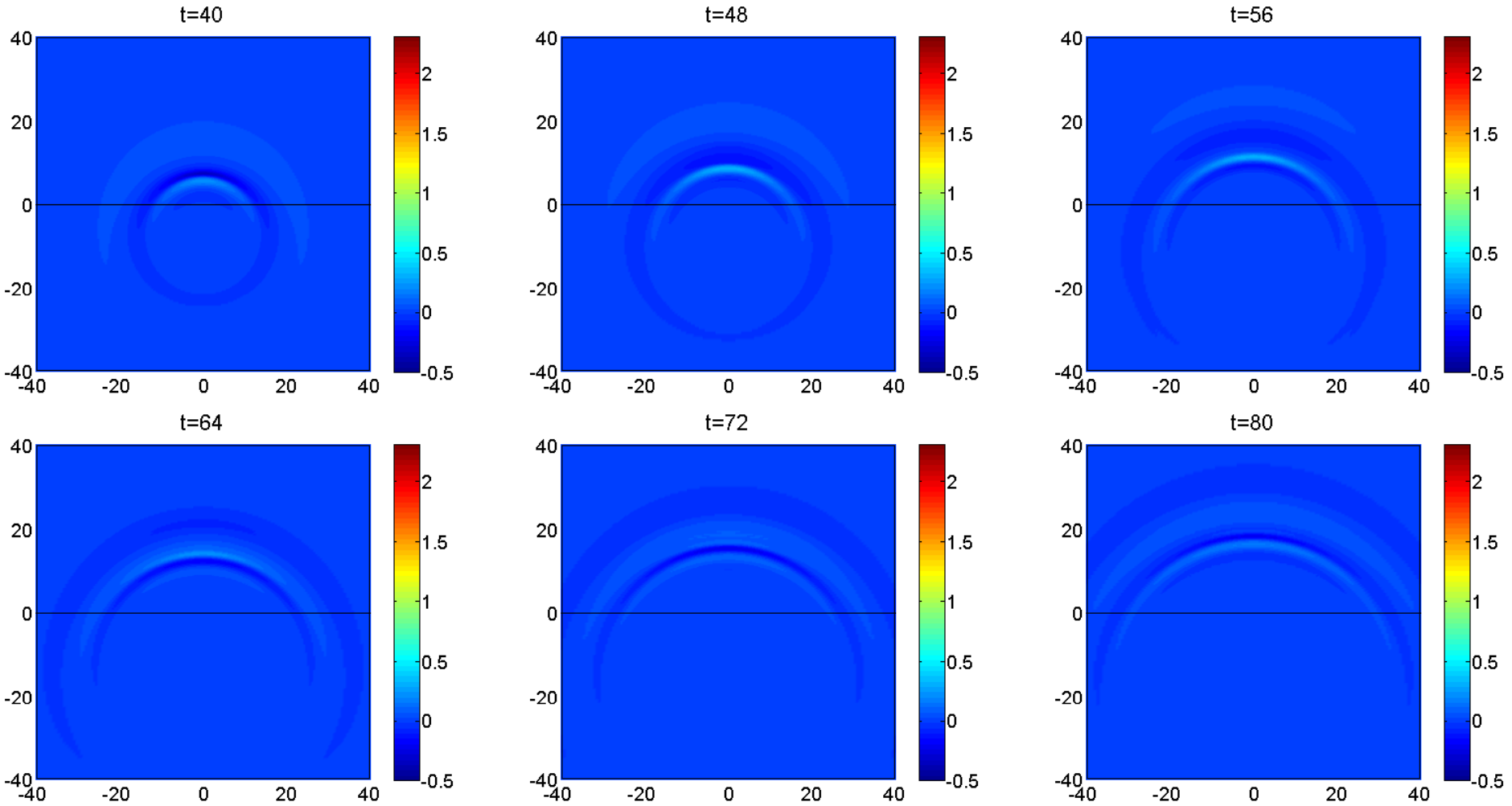

Figure 7: Evolution of the solution for $c = 0.27$, moving frame, central differences approximation of w_{tz}, larger region $[-200, 200]^2$, larger times.

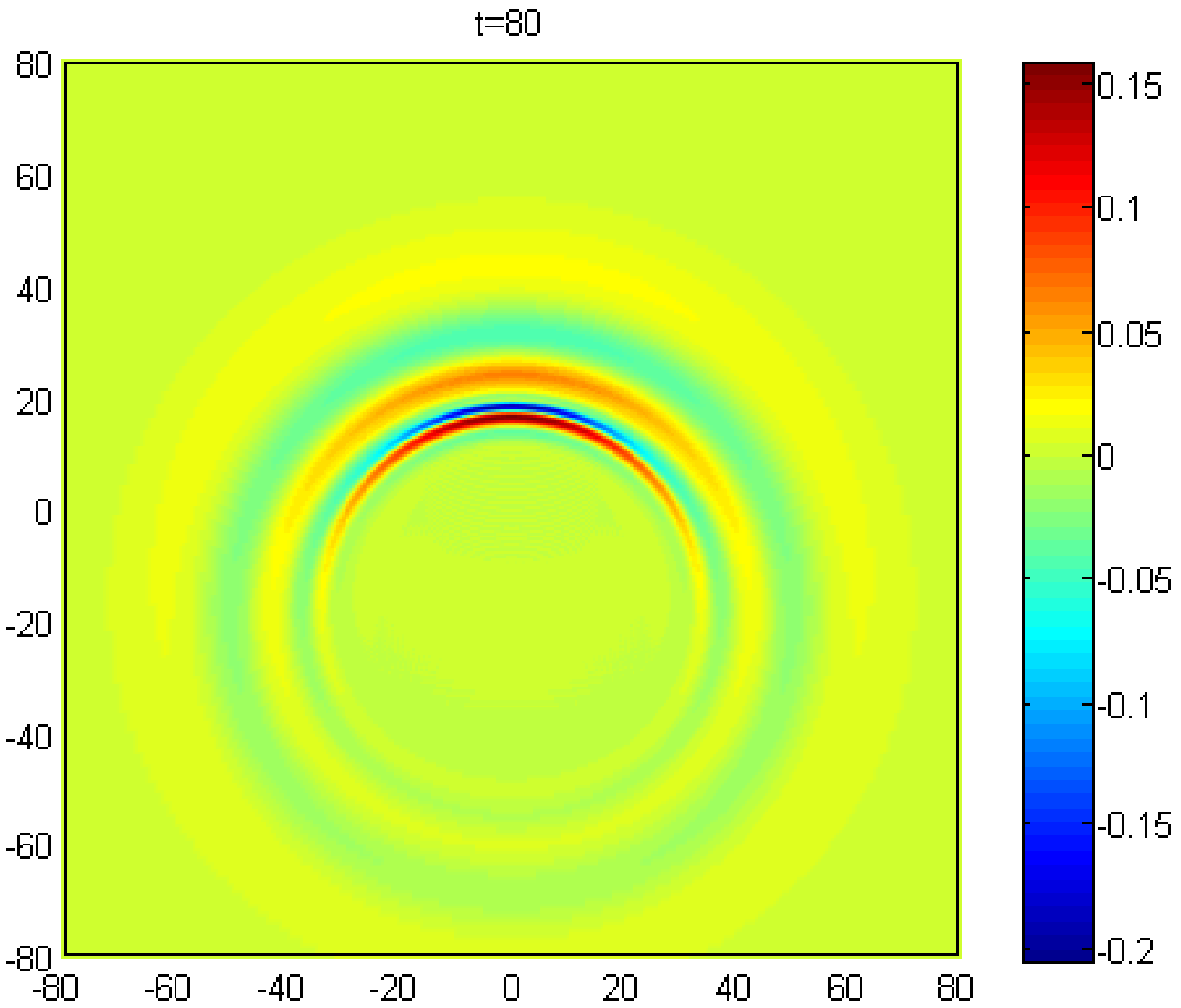

Figure 8: Evolution of the solution for $c = 0.27$, moving frame, central differences approximation of w_{tz}, $t = 80$, larger region $[-200, 200]^2$, different colormap.

Example 2. The second case is for a phase speed $c = 0.28$. The grid has 161×161 points in the region $[-20, 20]^2$, $\tau = 0.1$. For $t < 10$ the solution stays near the center of the moving frame coordinate system and behaves like a soliton, i.e., preserves its shape, although its maximum slightly varies. For larger times the solution turns to grow and blows-up for $t \approx 20$. The values of the maximum of the solution $u_{\max}$ and the trajectory of the maximum $y_{\max}$ are shown in Fig.9. The results in the next figures are for fixed coordinates (Fig.10), for moving frame with upwind approximation of w_{tz} (Fig.11), with central differences approximation of w_{tz} (Fig.12), for finer grid with 321×321 points and $\tau = 0.05$ (Fig.13).

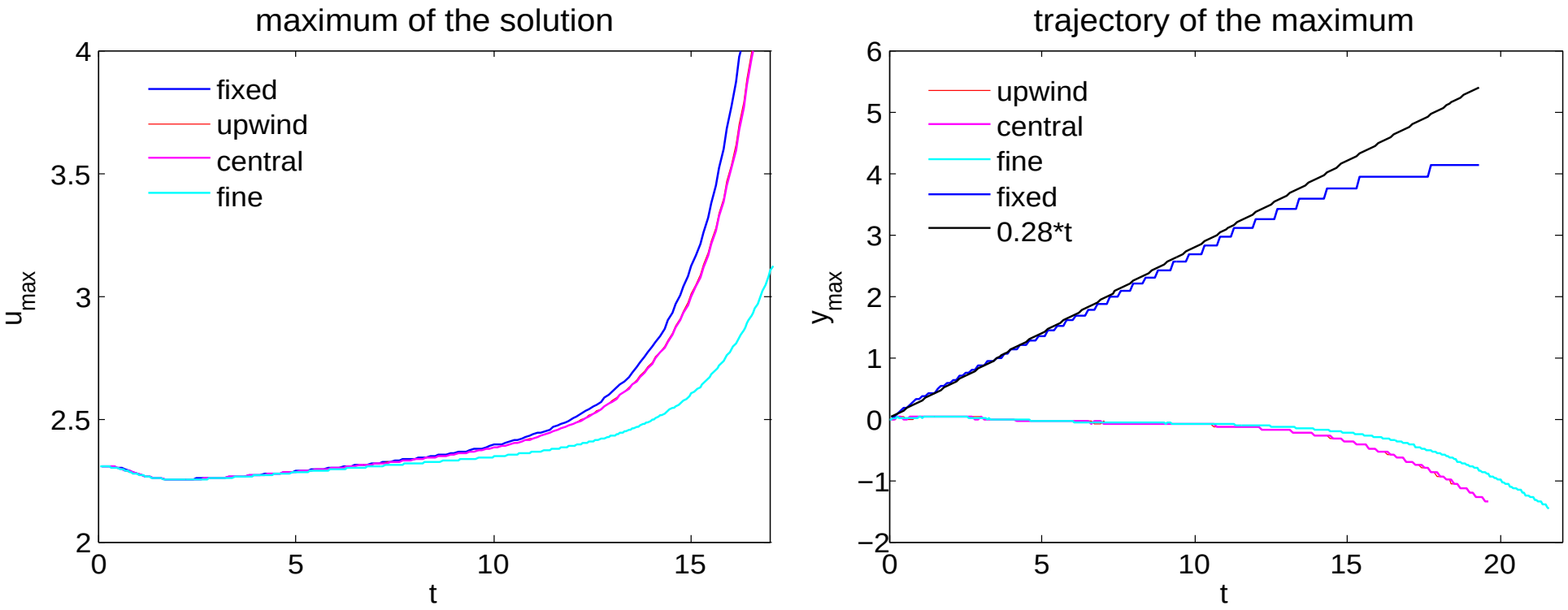

Figure 9: Evolution of the solution for $c = 0.28$ – the values and the trajectory of the maximum

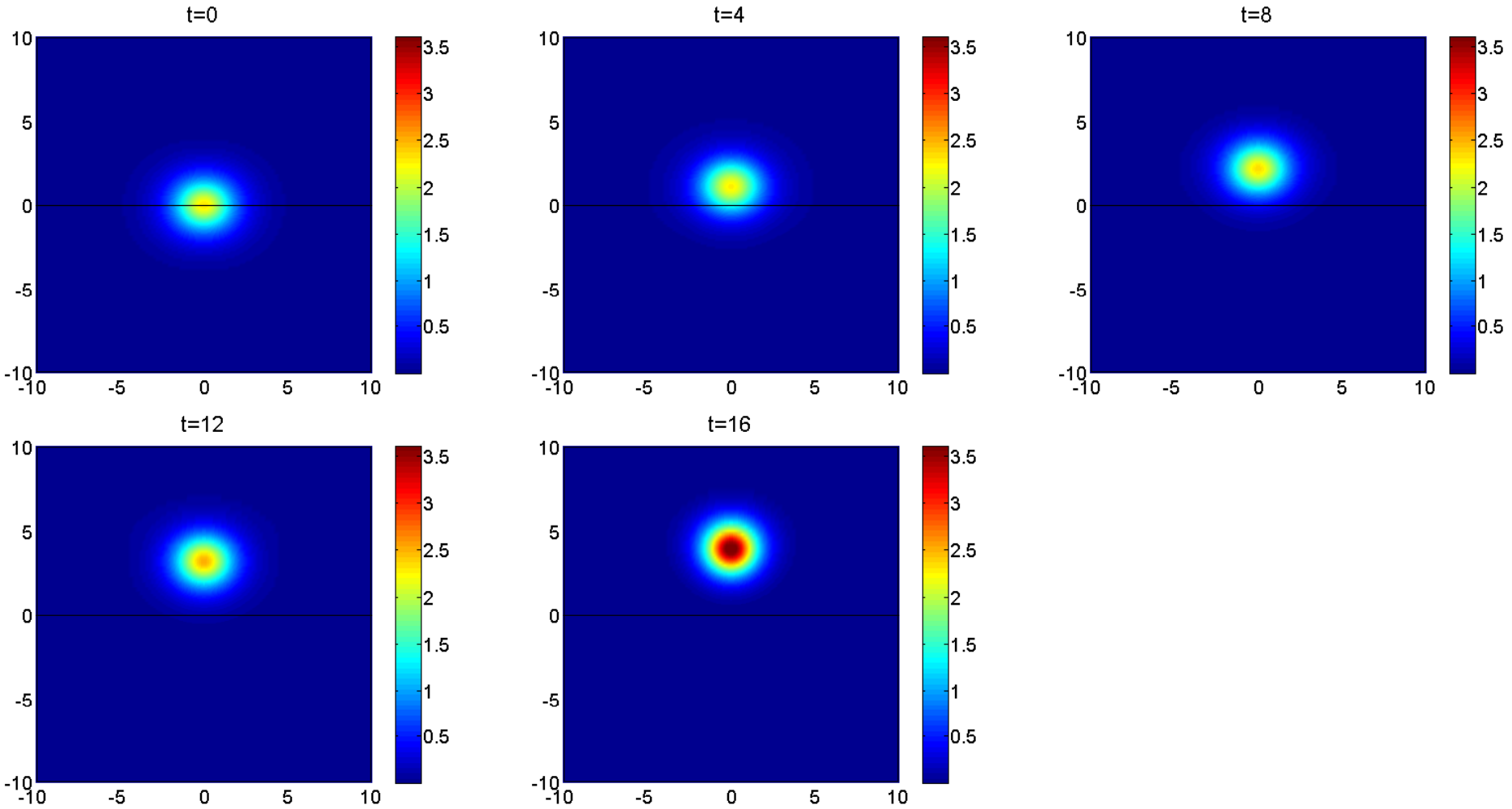

Figure 10: Evolution of the solution for $c = 0.28$, fixed coordinate system, grid with 161×161 points in $[-20, 20]^2$, $\tau = 0.1$.

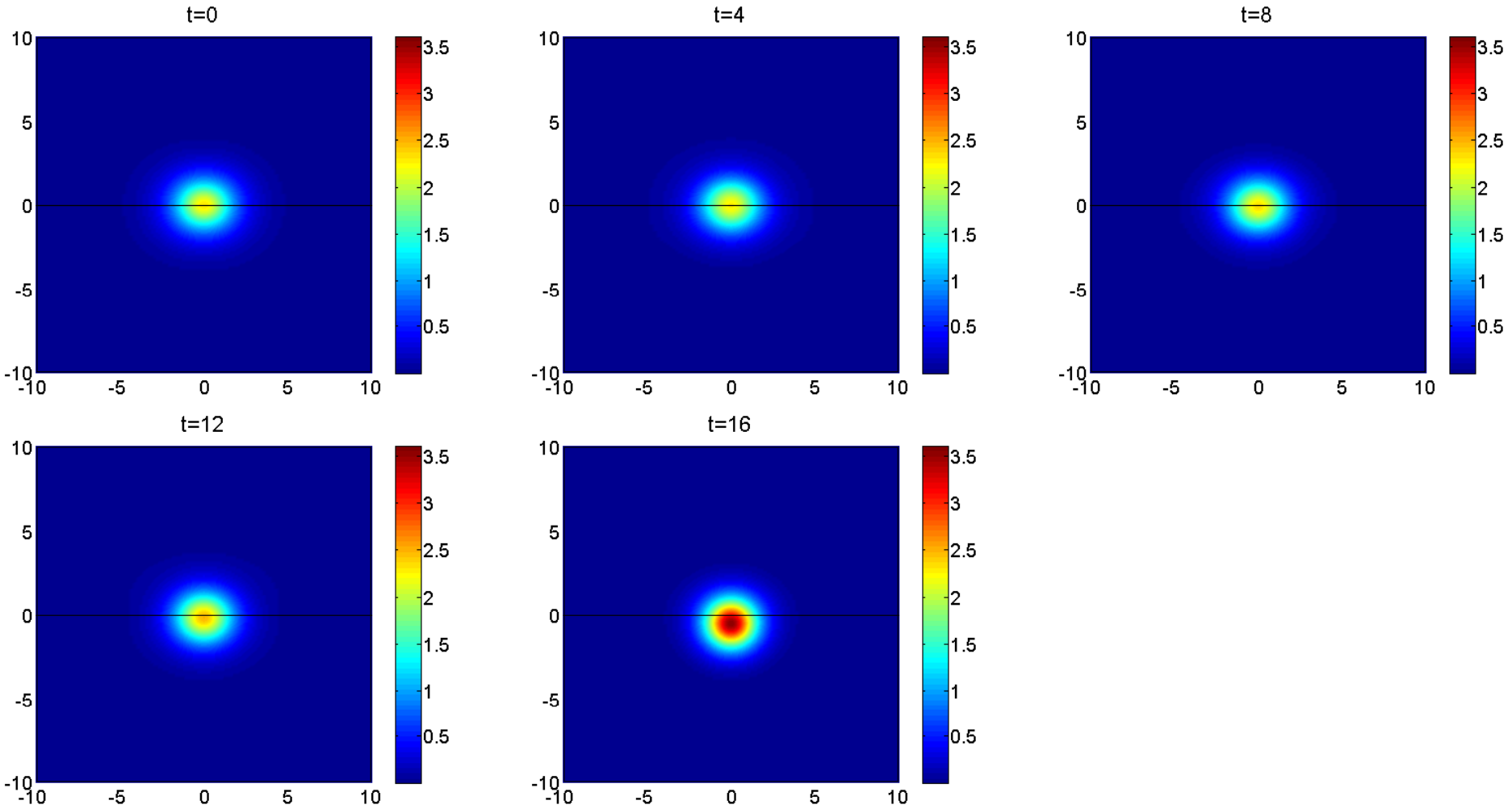

Figure 11: Evolution of the solution for $c = 0.28$, moving frame, upwind approximation of w_{tz}, grid with 161×161 points in $[-20, 20]^2$, $\tau = 0.1$.

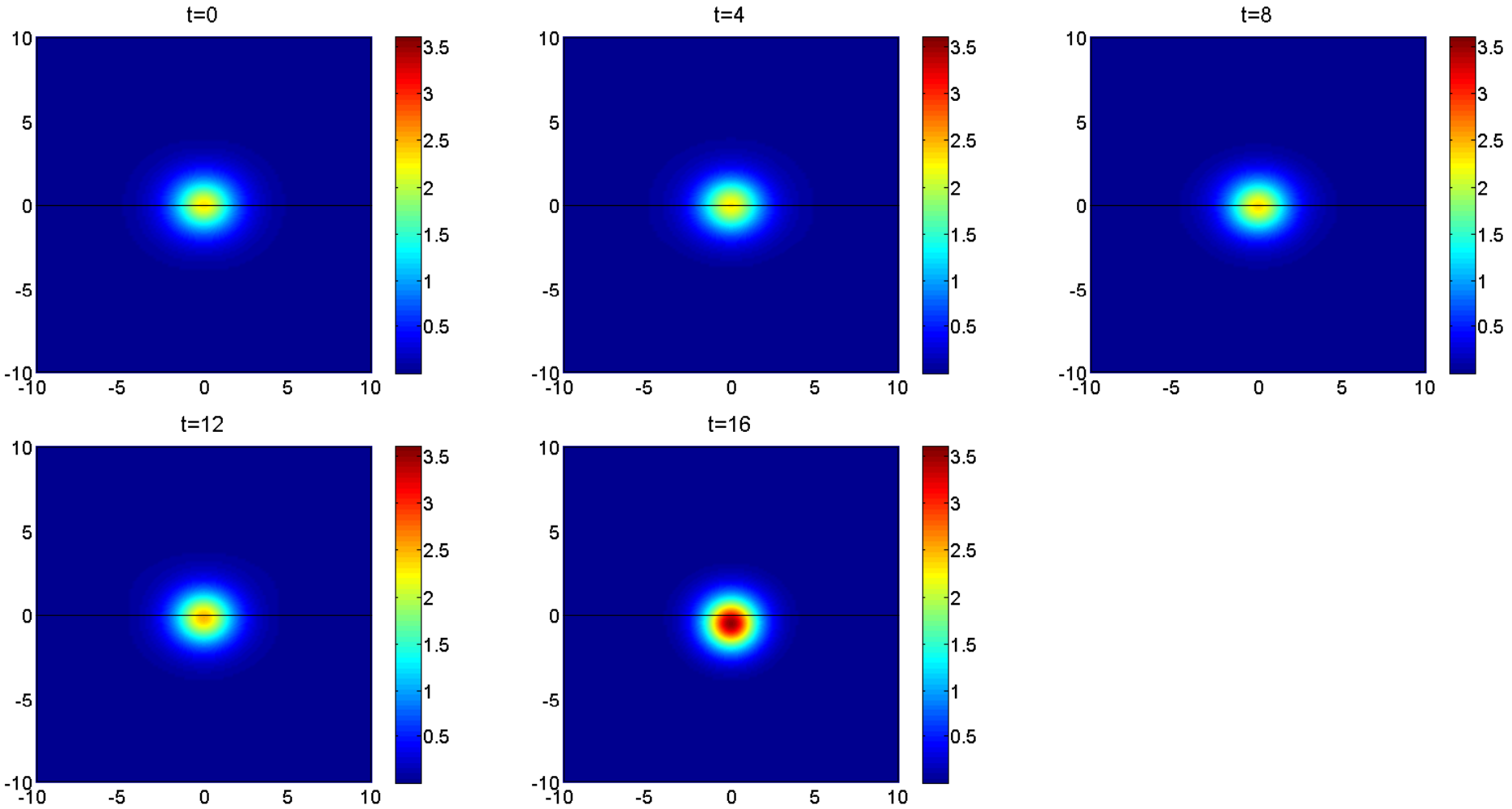

Figure 12: Evolution of the solution for $c = 0.28$, moving frame, central differences approximation of w_{tz}, grid with 161×161 points in $[-20, 20]^2$, $\tau = 0.1$.

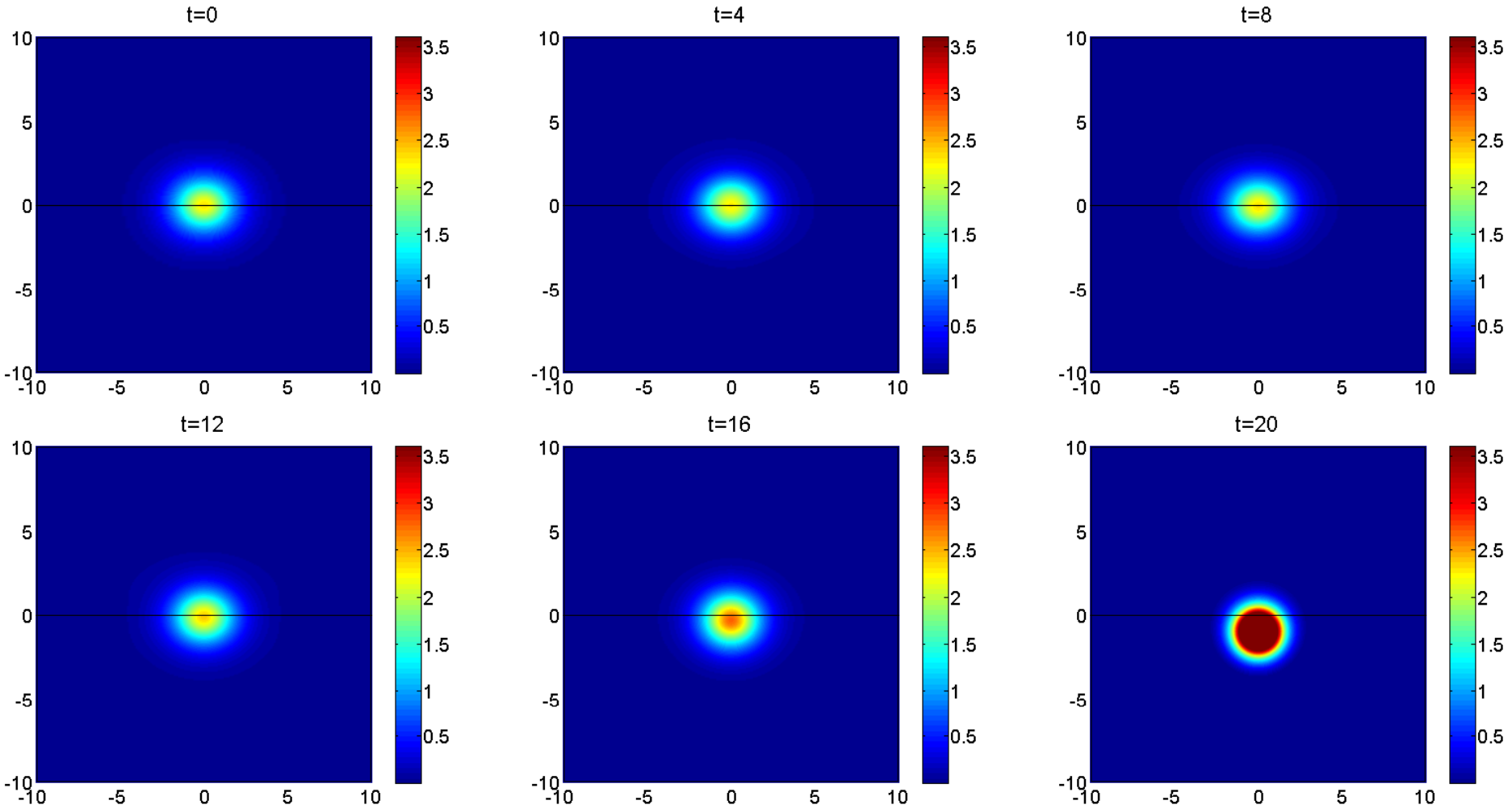

Figure 13: Evolution of the solution for $c = 0.28$, moving frame, central differences approximation of w_{tz}, finer grid with 321×321 points in $[-20, 20]^2$, $\tau = 0.05$.

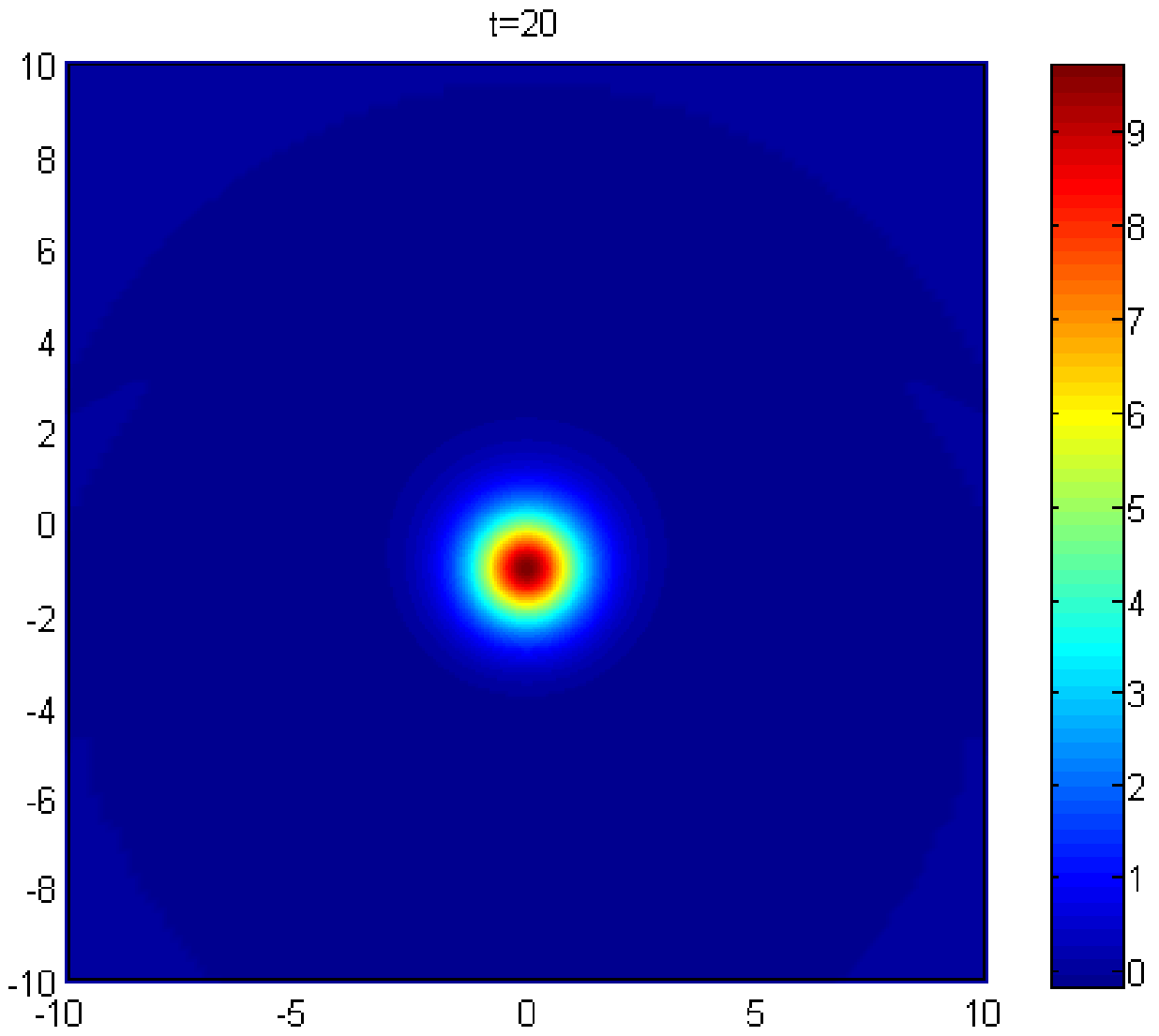

Figure 14: Evolution of the solution for $c = 0.28$, moving frame, central differences approximation of w_{tz}, finer grid, different colormap

Example 3. The initial data are

$$u(x,y,0) := u^{\text{sech}}(x) = 1.5\frac{1-c^2}{\alpha}\text{sech}^2\big(0.5\sqrt{\frac{1-c^2}{\beta_2-\beta_1 C^2}}\,x\big).$$

The boundary conditions on $y=-20$ and $y=20$ are taken as

$$u(x,\pm 20,t) := u^{\text{sech}}(x).$$

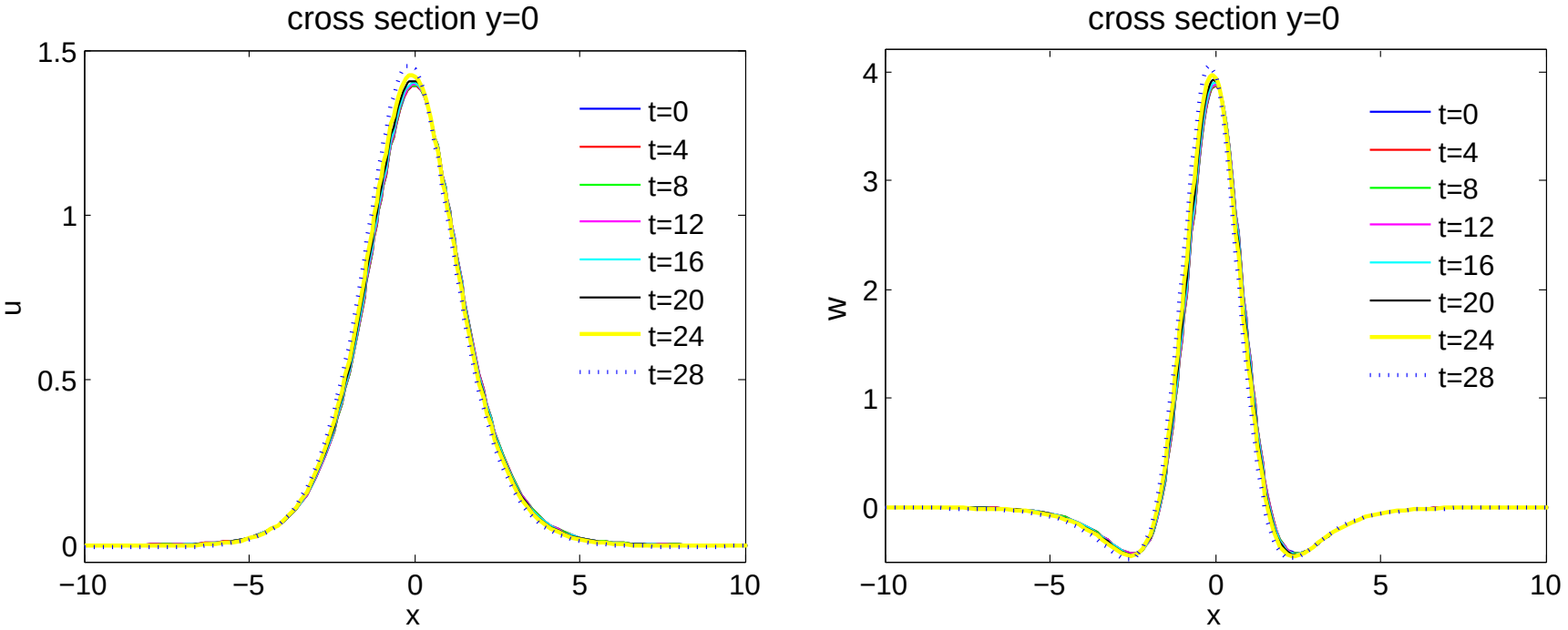

Figure 15: Evolution of the solution for $c=0.27$, moving frame, central differences approximation of w_{tz}

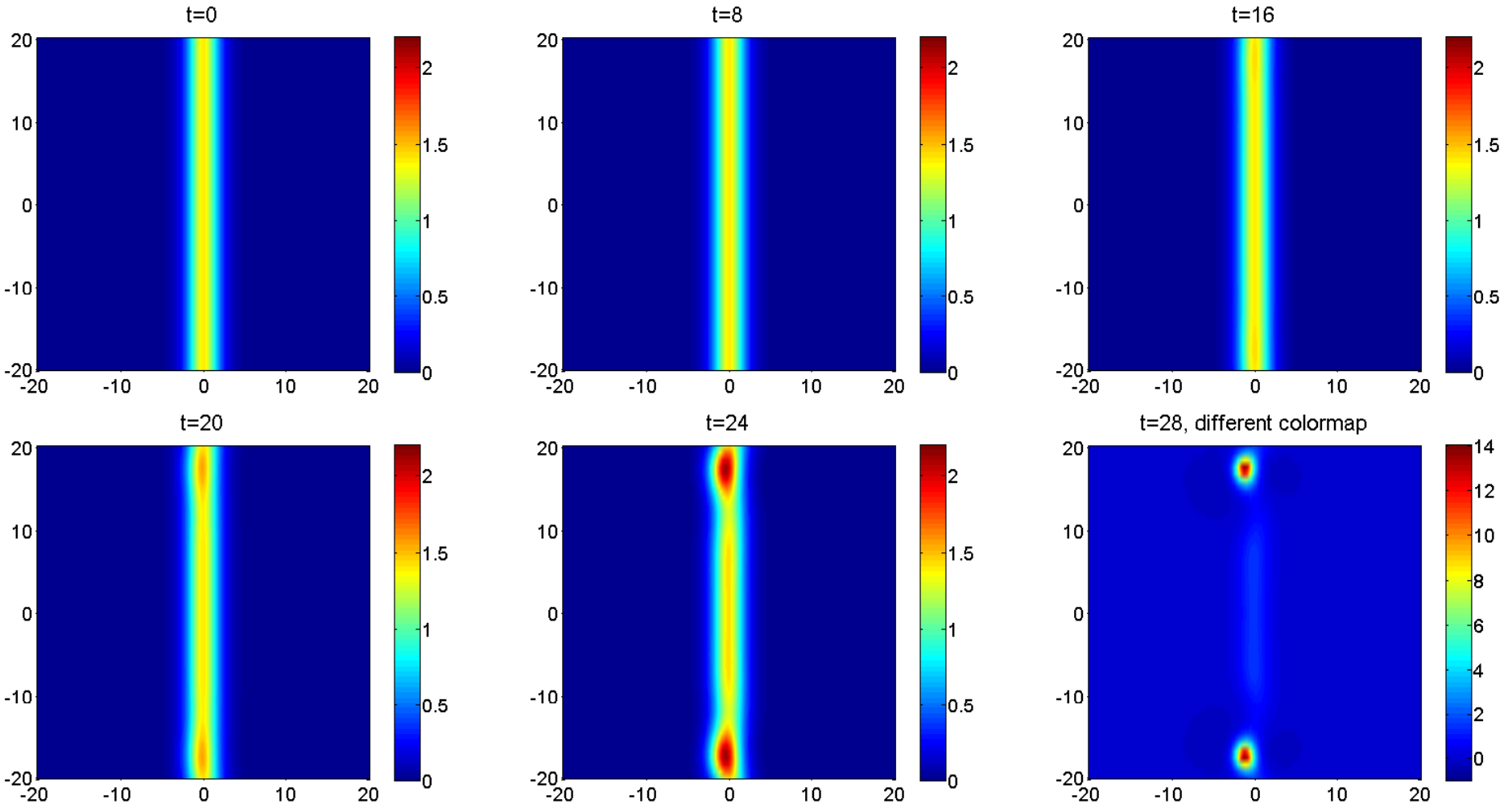

Figure 16: Evolution of the solution, $c = 0.27$, grid with 161×161 points in $[-20, 20]^2$, $\tau = 0.1$.

Table 1: Convergence in space and time, $c = 0.27$

		$t = 4$				$t = 8$				$t = 12$			
τ	$N_x{+}1$	$\max\lvert u{-}u^{\text{sech}}\rvert$	α	$\max\lvert(u{-}u^{\text{sech}})(\cdot,0)\rvert$	α	$\max\lvert u{-}u^{\text{sech}}\rvert$	α	$\max\lvert(u{-}u^{\text{sech}})(\cdot,0)\rvert$	α	$\max\lvert u{-}u^{\text{sech}}\rvert$	α	$\max\lvert(u{-}u^{\text{sech}})(\cdot,0)\rvert$	α
		second IC according to $\partial u/\partial t = 0$, central differemce approximation of u_{tz}											
0.1	160	1.37e-3		1.10e-3		5.06e-3		2.51e-3		1.70e-2		4.76e-3	
0.05	320	3.58e-4	1.94	2.81e-4	1.97	1.32e-3	1.94	6.38e-4	1.98	4.45e-3	1.93	1.21e-3	1.98
		second IC according to $u(x,z,-\tau) = u^s(x,z;c)$, central differemce approximation of u_{tz}											
0.1	160	1.36e-3		1.09e-3		5.04e-3		2.49e-3		1.70e-2		4.74e-3	
0.05	320	3.56e-4	1.93	2.79e-4	1.97	1.32e-3	1.93	6.36e-4	1.97	4.44e-3	1.94	1.21e-3	1.97
		second IC according to $u(x,z,-\tau) = u^s(x,z;c)$, upwind approximation of u_{tz}											
0.1	160	1.36e-3		1.09e-3		5.04e-3		2.49e-3		1.70e-2		4.75e-3	
0.05	320	3.56e-4	1.93	2.79e-4	1.97	1.32e-3	1.93	6.37e-4	1.97	4.44e-3	1.94	1.21e-3	1.97
		second IC according to $u(x,z,-\tau) = u^s(x,z;c)$, fixed grid											
0.1	160	1.81e-3		1.61e-3		6.78e-3		4.09e-3		2.42e-2		9.02e-3	
0.05	320	4.69e-4	1.95	4.03e-4	2.00	1.75e-3	1.95	1.08e-3	1.92	6.21e-3	1.96	2.27e-3	1.99
		second IC according to $\partial u/\partial t = 0$, central/upwind approximation of u_{tz}, uniform grid											
0.1	160	1.05e-2		8.95e-3		3.36e-2		1.79e-2		1.13e-1		3.17e-2	
0.05	320	2.66e-3	1.98	2.24e-3	2.00	8.41e-3	2.00	4.44e-3	2.01	2.74e-2	2.04	7.84e-3	2.02
		second IC according to $\partial u/\partial t = -c\,\partial u^s/\partial y$, fixed uniform grid											
0.1	160	1.00e-2		7.12e-3		2.82e-2		1.25e-2		8.61e-2		1.64e-2	
0.05	320	2.56e-3	1.97	1.45e-3	2.30	7.18e-3	1.97	3.19e-3	1.97	2.15e-2	2.00	4.23e-3	2.00

The table shows second order convergence. On the coarse grid the solution blows-up for $t \approx 30$, on the fine grid – for $t \approx 35$. The blow-up time is less for the fixed grid computations. On the coarse uniform grid the solution blows-up for $t \approx 23$, on the fine – for $t \approx 28$. The blow-up time is greater for the fixed grid computations.

Conclusions

- The results confirm the solitonic-like behaviour of the solutions for relatively small times.
- Unfortunately, the investigated solutions are not structurally stable and transform either in diverging propagating waves or blow-up.
- For $c \approx 0.28$, an time interval exists in which the solution is virtually preserving its shape whils steadily translating means that 2D solitons could be found for equations from the class of the BPE. This means that the nonlinearity is strong enough to balance the dispersion which is now much stronger than in the 1D case.
- Probably, the quadratic nonlinearity in BPE is not enough for modeling permanent soliton-like waves. Our future plans include experiments with different types of nonlinearities in the source term and in the coefficients of the equation.
- The moving frame coordinate system allows us to keep the localized structure in the center of coordinate system, where the grid is much finer, and to reduce the effects of the reflection from the boundary.